Available online at www.sciencedirect.com
SCIENCE DIRECT®
Ultrasonics 41 (2003) 415–419
Ultrasonics
www.elsevier.com/locate/ultras

Simulation of RF data with tissue motion for optimizing stationary echo canceling filters

M. Schlaikjer [a,*], S. Torp-Pedersen [b], J.A. Jensen [a]

[a] Center for Fast Ultrasound Imaging, Ørsted·DTU, Build. 348, Technical University of Denmark, DK-2800 Kgs. Lyngby, Denmark
[b] Department of Rheumatology, Parker Institute, Frederiksberg Hospital, Nordre Fasanvej 57, DK-2000 Frederiksberg, Denmark

Received 27 March 2003; received in revised form 9 May 2003; accepted 26 May 2003

Abstract

Blood velocity estimation is complicated by the strong echoes received from tissue surrounding the vessel under investigation. Proper blood velocity estimation necessitates use of a filter for separation of the different signal components. Development of these filters and new estimators requires RF-data, where the tissue component is known. In vivo RF-data does not have this property. Instead simulated data incorporating all relevant features of the measurement situation can be employed. One feature is the motion in the surrounding tissue induced by pulsation, heartbeat, and breathing. This study has developed models for the motions and incorporated them into the RF simulation program Field II, thereby obtaining realistic simulated data. A powerful tool for evaluation of different filters and estimators is then available. The model parameters can be varied according to the physical situation with respect to scan-site and the individual to be scanned. The nature of pulsation is discussed, and a relation between the pressure in the carotid artery and the experienced vessel wall motion is derived.

Keywords: Ultrasound; Tissue motion; Blood velocity estimation; RF-data simulation; Field II

1. Introduction

Ultrasound for cardiovascular imaging is widely used today for diagnostic purposes. From recorded RF-signals estimates of the velocity distribution of the blood flow can be computed, which can reveal cardiovascular diseases such as occlusions. Use of simulated RF-data is desirable, when developing new blood velocity estimators, stationary echo canceling filters, and other filters for processing recorded RF-signals, since they are well defined. In vivo RF-signals do not have this property, since the signal components from the surrounding tissue and the blood are not easily distinguishable, and the exact extend of the vessel is unknown.

To obtain realistic simulated RF-data all relevant features of the measurement situation must be incorporated. One feature is the motion in the tissue surrounding the vessel under investigation induced by breathing, heartbeat, and pulsation of arterial vessel walls. The motion is a result of a change in position of one or more organs (lung and heart), and vessel walls, whereby motion is induced upon adjacent tissue regions. Our previous study [1] investigated the presence of the different motion contributors and the modeling here of, and resulted in three models describing the temporal and spatial varying contributions to the total motion from pulsation, breathing, and heartbeat motion. The models were developed based on investigations of in vivo RF-data. Simulations for the carotid artery were performed and evaluated.

This study addresses improvement of the models to achieve better simulated RF-data. Investigations of the ability to model and simulate tissue motion in the abdominal region are performed, and the results are presented. To explain the nature of vessel dilation a mathematical relation between the dilation and the pressure in the carotid artery is derived.

All simulations are based on the Field II program [2] using spatial impulse response and point scatterers. This program can handle any array transducer, focusing, apodization, and transducer excitation.

* Corresponding author. Tel.: +45-45-253705; fax: +45-45-880117.
E-mail address: mas@oersted.dtu.dk (M. Schlaikjer).

0041-624X/03/$ - see front matter © 2003 Elsevier B.V. All rights reserved.
doi:10.1016/S0041-624X(03)00150-1

Table 1
Recording conditions for determination of motion due to pulsation (P), heart (H) and breathing (B)

Dataset	Vessel	Scan plane	Motion
C1	Carotid artery	Transverse scan angle 90°	P, B
HV1	Hepatic vein	Right liver lobe intercostal scan	B, H (P)
HV2	Hepatic vein	Right liver lobe intercostal scan	H (P)
HV3	Hepatic vein	Left liver lobe epigastric scan	H (P)

2. System and recording conditions

Modeling of the individual motions are based on investigation of in vivo RF-data recorded at different positions revealing the motion information. The measurements were performed with a 3.2 MHz probe on a B&K 3535 ultrasound scanner connected to a dedicated, real-time sampling system [3] capable of acquiring 0.27 s of data along one RF-line. The probe was hand-held, and data were obtained from 10 healthy volunteers. To cover the whole cardiac cycle each measurement was repeated 10 times, resulting in a data material consisting of 400 independent RF measurements of 950 pulse echo lines. No ECG synchronization could be performed, so it cannot be guaranteed that the whole cardiac cycle was covered in the complete measurement set for each volunteer.

Table 1 lists the scan sites and the motions present during measurements. The subjects were lying supine. For the HV1 recordings the subjects were breathing shallowly to keep the vessel within the Doppler gate. During recordings of the HV2 and HV3 data, the subjects were told to hold their breath.

3. Models developed from in vivo data

All models developed here and in [1] are based on investigation of the measured in vivo RF-data. The data were bandpass filtered to remove noise, and the autocorrelation method [4] applied to obtain estimates of the tissue velocities. Thirty-four adjacent RF-lines (temporally) were used to obtain high-quality estimates. Estimates of motion were obtained from the velocity estimates by summing over time at each depth. Plots of these estimates as a function of time and depth reveals the information needed to develop the motion models. In [1] the presence of motion in the surrounding tissue was found, and therefore it must be incorporated into the simulation to obtain realistic simulated data. All motion generators contribute to the total motion in the surrounding tissue. The individual contributors are assumed independent, so the accumulated tissue motion at a given scan-site can be computed by adding the contributions from the individual motions present. The tissue velocities are in the mm/s range with amplitude levels depending on scan-site, motions present, and distance between scanned region and the motion generators. Thereby the levels of tissue and blood motion at the vessel wall are on the same order, making it difficult to distinguish the signal components belonging to tissue and blood respectively.

Figs. 1–3 show examples of dilation plots, which visualizes features of the different motions over time and depth. The dilation is positive, if the scatterers move towards the transducer relative to an initial position, and negative if movement is away from the transducer.

3.1. Pulsation

The pulsation in the arteries is due to the time varying pressure in the vessel during a cardiac cycle, and results in a force acting on the vessel walls. A radial motion of

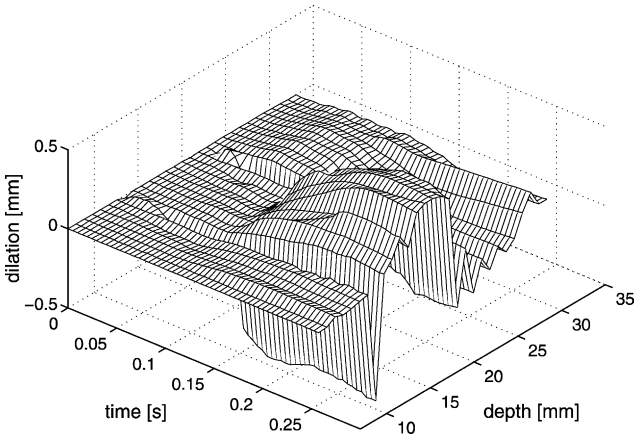

Fig. 1. Example of dilation found from in vivo data from the carotid artery. Pulse rate: 70 bpm.

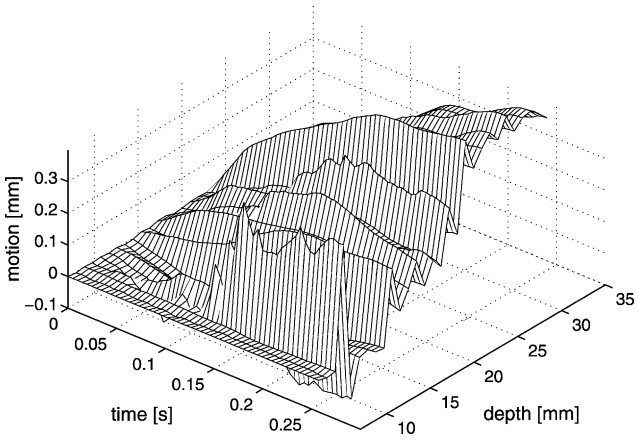

Fig. 2. Example of breathing motion at carotid artery.

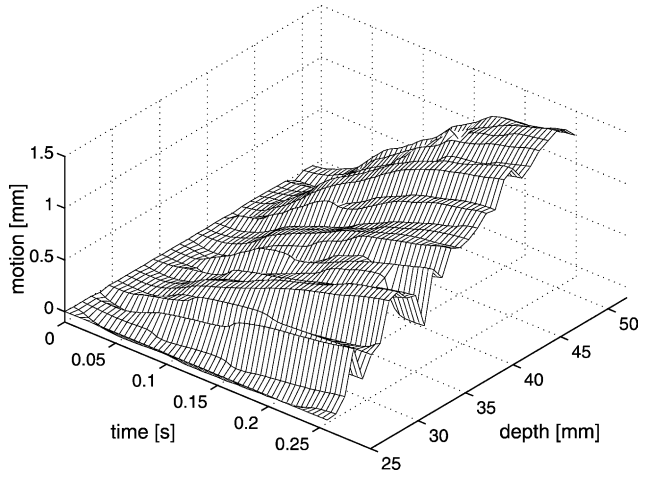

Fig. 3. Example of motion due to heartbeat (HV3) at hepatic vein.

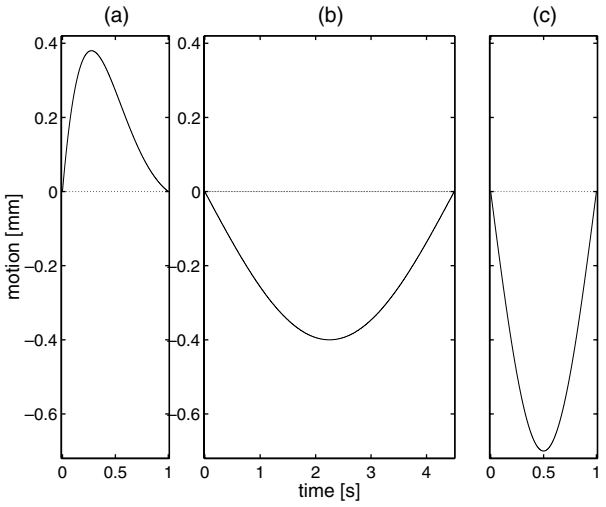

Fig. 4. Models of dilation due to pulsation (a), breathing (b) and heartbeat (c). Frequency of breath: 13 breaths/min, pulsation and heartbeat: 60 pulses/min.

the wall and the surrounding tissue [5] is induced. The pressure levels throughout a cardiac cycle in the carotid artery vary between 80 and 160 mmHg. The relation between the dilation, d, and the pressure, p, can be approximated by a parabola [6,7] as stated in Eq. (1), where p_0 is the diastole pressure and K a constant that accounts for the tissue characteristics. Eq. (1) has been derived from excised arteries (mostly dog arteries), but is assumed to hold for in vivo human arteries with proper choice of the tissue parameter K [8]:

$$d = \sqrt{\frac{p(t) - p_0}{K}} = \sqrt{\frac{\Delta P}{K}} \tag{1}$$

In Fig. 1 dilation estimates due to pulsation in the carotid artery are visualized. Due to the radial nature of pulsation two dilation sequences moving in opposite directions relative to the center of the vessel occurs. The figure reveals the onset of a cardiac cycle and thereby dilation at time equal to 0.12 s. The preceding estimates reveal the dilation, when returning to diastolic conditions. The time sequence of the dilation rises fast and then decreases and returns to the initial value. All motion is relative to the center of the vessel, and the level of motion is damped with increased radial distance. The motion therefore is a function of time and depth, and assuming no correlation between time and depth the motion model becomes a product of two functions—one describing the time sequence, and the other describing the depth dependence. In Fig. 4(a) the temporal model for dilation due to pulsation for a given depth is shown with a pulse rate of 1 pulse/s. The temporal sequence agrees with the in vivo dilation estimates obtained by Bonnefous [9].

In [1] the damping was modeled as a linear function of radius, which is not optimal. An exponential damping function, as given in Eq. (2), should be applied, where rd is the damping level at a given radius r, b a constant, R_w the radius of the vessel, and R_l, the maximum radial distance at which motion will be seen. Beyond R_l the damping function is equal to zero:

$$rd = b\left(\cos\left(\pi\frac{r - R_w}{R_l - R_w}\right) + 1\right) \quad \text{for } R_w < r < R_l \tag{2}$$

3.2. Breathing

Fig. 2 shows an example of motion due to breathing during inhalation. The lung "pushes" the tissue towards the transducer due to the location of the lung beneath the scan-site. The damping decreases with increasing depth. Again the motion is a function of time and space (as with pulsation). The repetition frequency will most often be lower, since the respiration frequency is lower than the heartbeat frequency. The time sequence at a given depth is shown in Fig. 4(b). The model has a negative sign, since the motion is acting in the opposite direction of the positive axial axis (z-axis).

3.3. Heartbeat

Fig. 3 shows an example of motion estimates due to the heart beating. It contains the same features as for breathing regarding position of motion generator, damping, and time sequence, but the repetition frequency is higher (in average 1 beat/s). The contractions have been shown not to follow the same temporal sequence as pulsation, and are assumed to be due to the more complex motion pattern (translation as well as rotation) of the heart. The model for the tissue motion is given in Fig. 4(c), again assuming that the motion is acting in the axial direction.

All the models contain the same features regarding time and depth dependence, but the repetition time,

amplitude, and damping vary with scan site and for the individual motion types. Additionally these model parameters vary among individuals.

4. Simulations of motion

The ability to create realistic simulated data incorporating the motion has been verified for the carotid artery and the hepatic vein (HV3). The transducer was modeled as a 3.2 MHz convex, elevation focused array. A focusing and apodization scheme matching the used scan probe was incorporated. As a result of the focusing settings a total of 58 elements were active in the aperture during transmission and receive. The point scatterers were given amplitude properties of tissue or blood, and moved around according to the motion model between each simulation of an RF-line. Womersley's pulsatile blood flow model [10] was used to determine the motion of the blood scatterers in the carotid artery. RF-data resembling 5 s were simulated to obtain data including the full effect from breathing and pulsation. Fig. 5 shows an example of simulated dilation for the carotid artery. The damping was modeled by Eq. (2), with R_l equal to 20 mm. The scan angle was 90°. Comparing with Fig. 1 reveals a good agreement between the two dilations. The pulse rates differ for the two situations, giving a faster pulsation sequence for the higher pulse rate. In Fig. 1 some motion is present within the vessel (center of vessel at depth equal to 19 mm)—probably because the scan angle was not exactly 90°, so that the blood influences the motion estimates.

The blood flow in the hepatic vein can be modeled by a steady flow superimposed a time varying, low amplitude flow. In the HV3 simulations only the heartbeat motion is present, requiring only 1 s of simulations to create RF-data covering a full cycle. The damping was

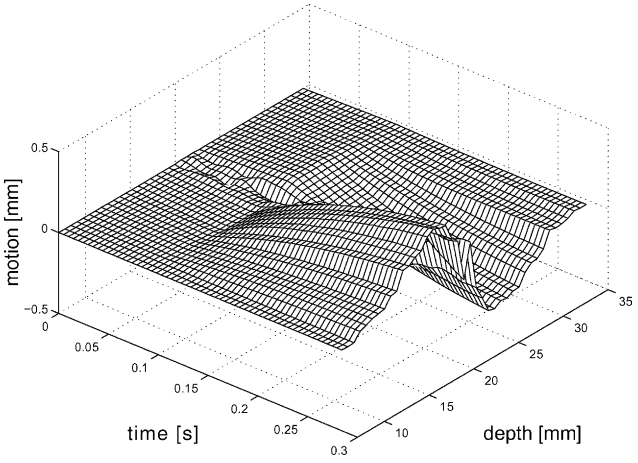

Fig. 5. Estimates of dilation from simulated data mainly due to pulsation at the carotid artery. Pulse rate: 60 bpm.

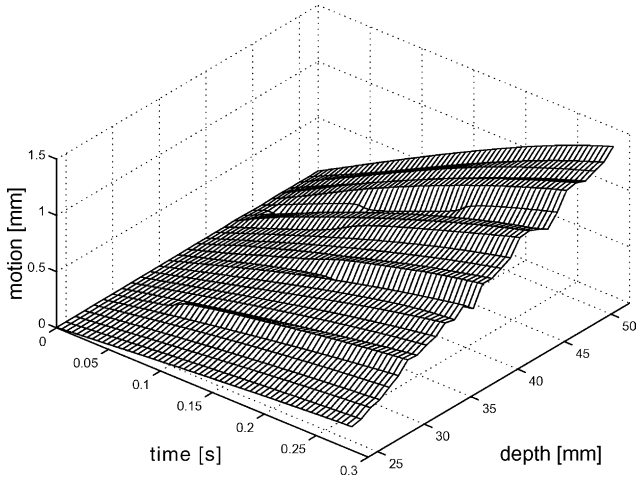

Fig. 6. Motion estimates based on simulated data resembling the HV3 recordings (motion is due to the beating of the heart). Pulse rate: 60 bpm.

modeled as a linear function of axial distance (z) with increasing amplitude for increased depth. The result of simulation is plotted in Fig. 6, and is to be compared with Fig. 3. The pulse rate for the real data is higher than for the simulated data, giving a faster motion sequence. Comparison reveals a good agreement between the motions, and simulation of realistic data for the abdominal region is thus possible.

5. Conclusions

The results presented here and in [1] prove presence of tissue motion. Motion models for each of the contributors have been developed and incorporated into the simulation program Field II. The generated simulated RF-data agrees well with in vivo RF-data. Thereby a powerful tool for optimization of filters and estimators for processing of RF-signals have been obtained. The model parameters (amplitude, repetition frequency) vary depending on scan-site, motions present and the individual to be scanned. All of these can be modified in the program. A simple equation describing the relation between pressure and the dilation in the carotid artery has been derived, which explains the nature of the motion due to pulsation.

Acknowledgements

This project is supported by grant 9700883 and 9700563 from the Danish Science Foundation, grant 980018-311 from the Technical University of Denmark, and by B-K Medical A/S, Denmark. Paul Stetson is acknowledged for his assistance with acquiring the in vivo RF-data.

References

[1] M. Schlaikjer, S. Torp-Pedersen, J.A. Jensen, P.F. Stetson, Tissue motion in blood velocity estimation and its simulation, in: Proc. 1998 IEEE Ultrasonics Symposium, 1998, p. 1495.
[2] J.A. Jensen, Users' guide for the Field II Ultrasound Simulation Program. Available from: <http://www.es.oersted.dtu.dk/staff/jaj/field>.
[3] J.A. Jensen, J. Mathorne, Sampling system for in vivo ultrasound images, in: Medical Imaging V Symposium, SPIE 1444, 1991, p. 221.
[4] C. Kasai, K. Namekawa, A. Koyano, R. Omoto, Real-time two-dimensional blood flow imaging using an autocorrelation technique, IEEE Trans. Son. Ultrason. 32 (1985) 458.
[5] W.W. Nichols, M.F. O'Rourke, McDonald's Blood Flow in Arteries, Theoretical, Experimental and Clinical Principles, Lea & Febiger, Philadelphia, 1990, pp. 77–124.
[6] J.D. Bronzino, The Biomedical Engineering Handbook, CRC Press, Boca Ranton, 1995, pp. 291–303.
[7] R. Skalak, S. Chien, Handbook of Bioengineering, McGraw-Hill Book Company, New York, 1987, pp. 16.1–16.28.
[8] J.O. Arndt, J. Klauske, F. Mersch, The Diameter of the Intact Carotid Artery in Man and its Change with Pulse Pressure, Plügers Arch. 301 (1968) 230–240.
[9] O. Bonnefous, Stenoses dynamics with ultrasonic wall motion images, in: Proc. 1994 IEEE Ultrasonics Symposium, 1994, p. 1709.
[10] D.H. Evans, Some aspects of the relationship between instantaneous volumetric blood flow and continuous wave Doppler ultrasound recordings III, Ultrasound Med. Biol. 9 (1982) 617.